MR. H.M. WOODNOOFFE

CANADA

DEPARTMENT OF ENERGY, MINES AND RESOURCES

OTTAWA

MINES BRANCH INVESTIGATION REPORT IR 69-49

FERRITES: PART IV. THE MAGNETIC AND CERAMIC PROPERTIES OF MIXED BARIUM-STRONTIUM FERRITES

by

SUTARNO, W. S. BOWMAN AND G. E. ALEXANDER

MINERAL SCIENCES DIVISION

COPY NO. 16

JULY 13, 1969

MINES BRANCH INVESTIGATION REPORT IR 69-49

FERRITES: PART IV. THE MAGNETIC AND CERAMIC PROPERTIES OF MIXED BARIUM-STRONTIUM FERRITES

by

Sutarno*, W.S. Bowman** and G.E. Alexander**

SUMMARY OF RESULTS

The ceramic and magnetic properties of mixed barium-strontium ferrites having the composition $(Ba_{1-x}Sr_x)O.5{\cdot}2\,Fe_2O_3$, where $0 \leq x \leq 1$ and $\Delta x = 0{\cdot}2$, have been studied. Anisotropic ferrite magnets with the above composition have been prepared and their green and sintered densities, diametral and thickness shrinkages, coercive force, remanent magnetization and maximum energy product have been measured and plotted as functions of their sintering temperatures and of their compositions. It was found that pure strontium ferrite ($x = 1$) has the best ceramic and magnetic properties in this system. An unexpectedly simple relationship was found to hold between the intrinsic coercive force and the density of all specimens.

---

*Research Scientist and **Technical Officers, respectively, Mineral Sciences Division, Mines Branch, Department of Energy, Mines and Resources, Ottawa, Canada.

CONTENTS

INTRODUCTION

Hexaferrites having the chemical composition $MO.nFe_2O_3$, where M is Ba, Sr, Pb or a mixture thereof and n is either equal to or near 6·0, have been used successfully as the basic materials for the manufacture of ceramic permanent magnets. Not only can they be produced from relatively inexpensive raw materials, but also, this type of magnet has several properties that, for certain applications, are superior to those of metallic magnets. The ceramic permanent magnet has a high coercive force, high thermal and electrical resistivity and is chemically inert. At the same time, its maximum energy product $(BH)_{max}$ is still sufficiently high to be useful. The magnetic properties are derived from the anisotropic nature of the hexaferrite crystals. In order to take full advantage of this anisotropy, the crystallite particles of the ceramic magnet must be aligned so that their c-axes are parallel. This alignment can be obtained by the application of a magnetic field during the fabrication of the ceramic body (1)*.

Another important requirement for a good ceramic magnet is that it must be as dense as possible in order to have the greatest number of magnetic particles per unit volume, while, at the same time, its grain size must be maintained as small as possible in order to keep the coercive force high.

Various approaches have been used by a number of workers to prepare a dense, anisotropic, ceramic magnet with a small grain size. Some of their results have been summarized in an earlier report (2). Most investigators used the doping technique to improve the ceramic properties of the ferrite. A large number of elements have been reported to improve the properties of ceramic ferrite magnets. Some were added in order to lower the calcination temperature (3), while others were added as grain-growth inhibitors. Generally, all the efforts to improve the properties of

---

*For references, see pages 34 and 35.

ferrite permanent magnets have been concentrated on the improvement of the ceramic properties, hoping thereby simultaneously to improve the magnetic properties as such.

There are many variables that affect the ceramic properties of a ferrite magnet body. These variables can be divided into two main groups: (i) technological variables such as the method of preparation of the powder, calcination temperature, length of milling time, etc., and (ii) chemical variables, such as the Fe/M ratio, Ba:Sr:Pb proportions, and the concentration of minor constituents such as doping agents or impurities.

It is difficult to assess the importance of each of the variables individually to the final properties. Some of them, such as the Fe_2O_3/MO ratio (4), milling method and the particle size of the powder (5, 6), and method of preparation (7), have important effects on the properties of the ceramic magnet body. In this work, the effect of Ba/Sr ratio on the magnetic and ceramic properties of mixed barium-strontium hexaferrites has been investigated.

EXPERIMENTAL PROCEDURES

1. General Considerations

Several steps are required to prepare a ceramic magnet body (2). The effects of changes in some of these steps are inter-related. Ideally, one should study the effect of each variable on the properties of the product at each step. Because of the great number of variables involved in each step, an enormous volume of experimental work would be required. In the present work, in order to keep the volume of experimental work to a practical size, all the process variables were maintained as constant as possible. The only variation was in the Ba/Sr ratio. The powders were prepared by the same method, using materials from the same sources, with calcination at the same temperature, soaking time and heating rate, with milling for the same length of time under the same milling conditions. It will be understood that the results of the experiments are valid only for the particular conditions

outlined herein, and any extrapolation outside these conditions is hazardous. For any slight modification of the process variables, one must make an educated guess as to the outcome.

2. Sample Preparation

The materials used in this work were reagent-grade iron oxide, barium nitrate, strontium nitrate, ammonia and carbon dioxide gas. No further purification was carried out on these raw materials. The iron oxide and the barium and strontium nitrate solutions were assayed chemically by standard methods (8). The iron oxide was pre-dried at 150°C overnight. The experimental procedure is illustrated schematically in Figures 1A and 1B.

Appropriate amounts of iron oxide and barium/ strontium nitrate solution to make $Ba/Sr\ O.5 \cdot 2Fe_2O_3$ were mixed to form a slurry. The size of each batch was about 2·5 kg. The volume of the slurry was adjusted to about 20 litres by the addition of distilled water. The slurry was stirred vigorously and the pH was maintained at 8 during precipitation by introduction of ammonia gas. The precipitation was carried out by bubbling carbon dioxide gas into the slurry. The completion of the precipitation was indicated by a negative test of the supernatant liquid for barium/ strontium ions by means of both sulphate and carbonate methods (8).

After the completion of precipitation, the slurry was allowed to settle overnight and filtered through a Buchner filter on the following day.

The precipitate was then dried, and mixed manually in order to prepare it for calcination.

The calcination and milling schedules were as follows:

a. Calcination at 900°C for 1 hr.

b. Manual crushing in a mortar to about 30 mesh.

c. Calcination at 1100°C for 1 hr.

d. Manual mixing to pass 30 mesh.

e. Calcination at 1100°C for 1 hr.

f. Ball-milling of the whole batch in alcohol for 8 hr. to ensure

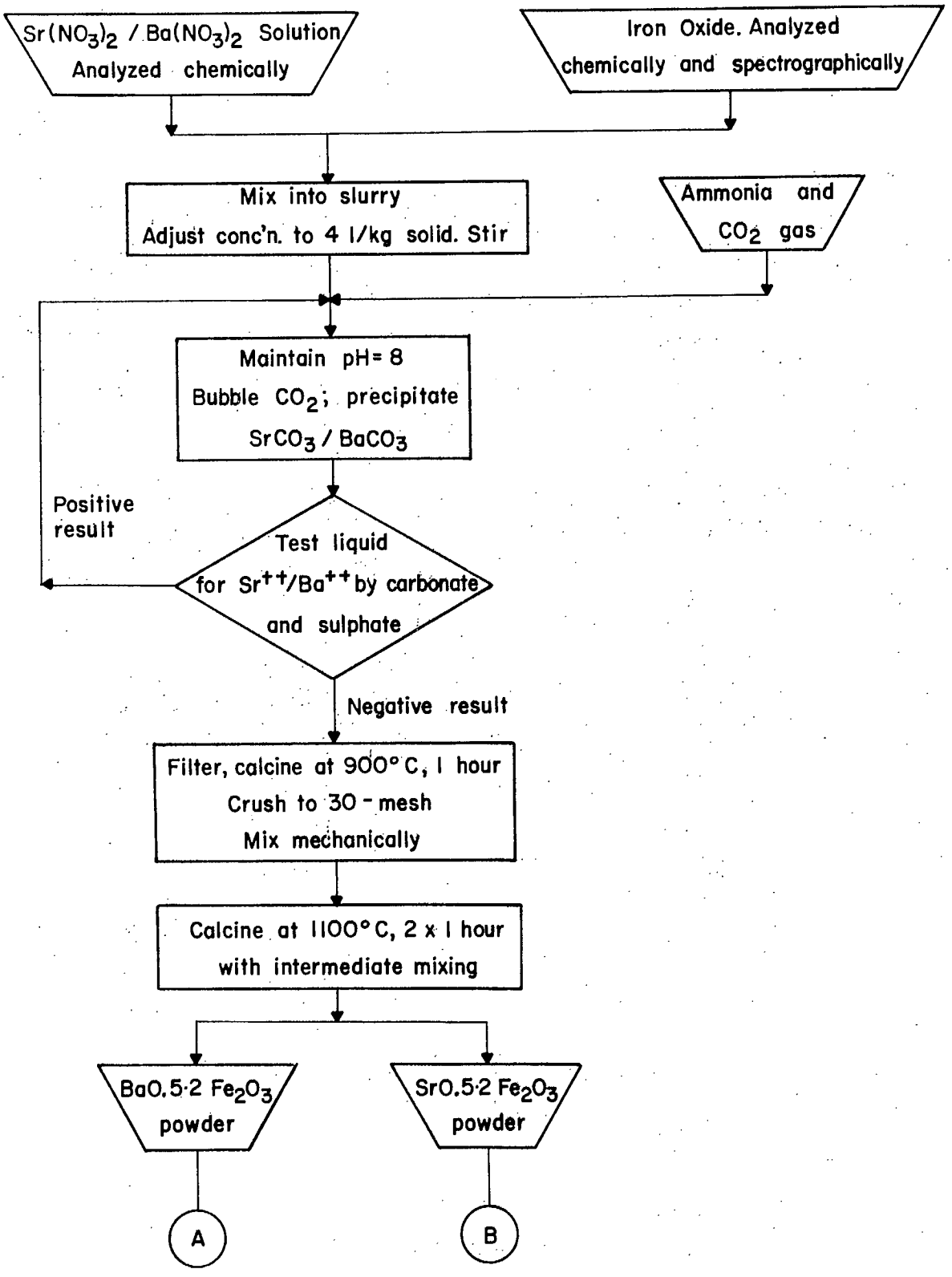

Figure 1A. Flow Sheet for Experimental Investigation of Ceramic and Magnetic Properties of Barium/ Strontium Ferrites (1st Section).

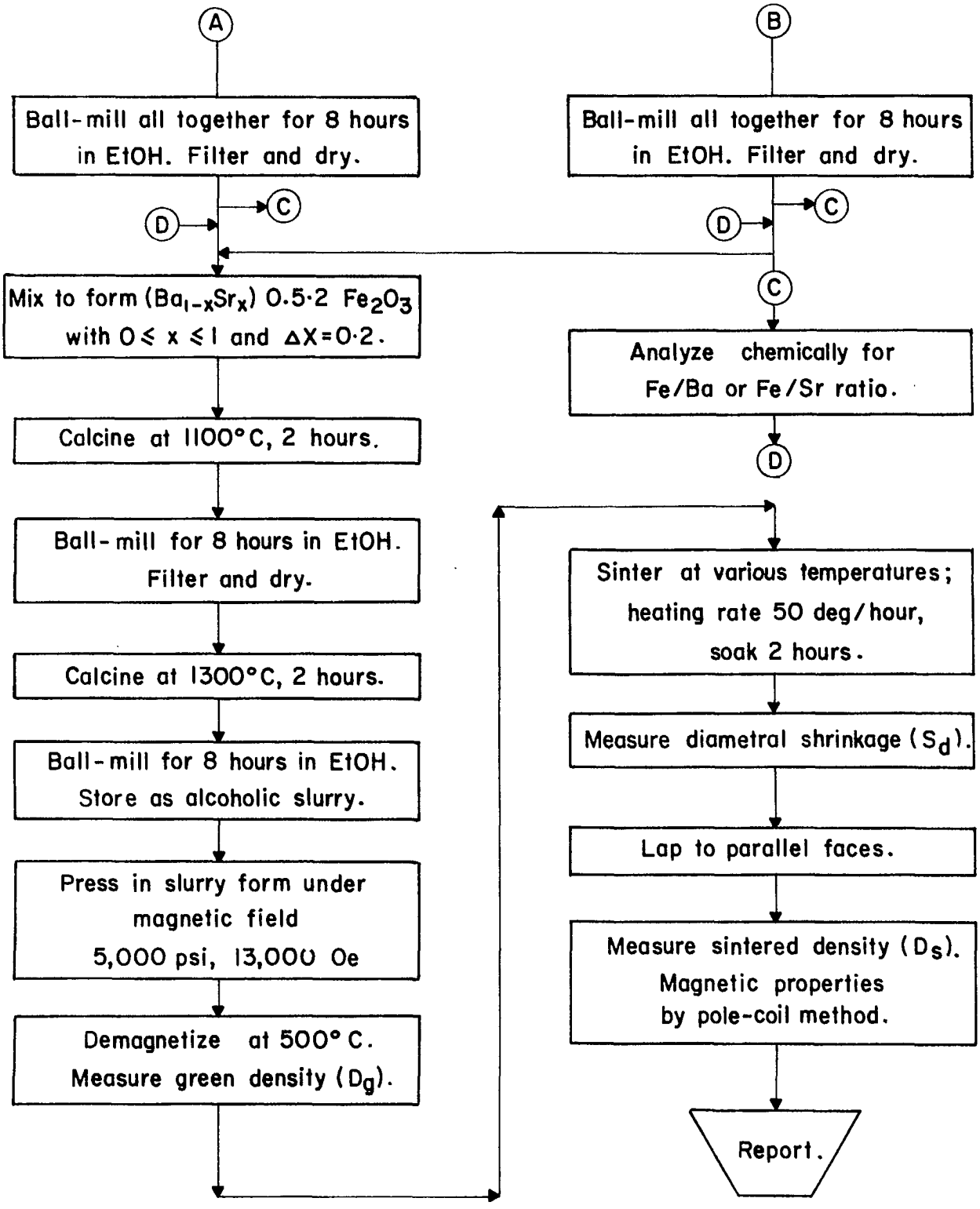

Figure 1B. Flow Sheet for Experimental Investigation of Ceramic and Magnetic Properties of Barium/ Strontium Ferrites. (2nd Section).

homogeneity, and subsequent drying at 110°C.

g. Mixing of barium and strontium ferrite powders to give $(Ba_{1-x}Sr_x)O.5{\cdot}2Fe_2O_3$ with $0 \leq x \leq 1$ and with $\Delta x = 0{\cdot}2$, where Δx is the composition interval.

h. Calcination of the mixture at 1100°C for 2 hr.

i. Ball-milling of the mixture in alcohol for 8 hr and subsequent drying at 110°C.

j. Calcination of the mixture at 1300°C for 2 hr.

k. Ball-milling of the mixture in alcohol for 8 hr and storage in the form of an alcohol slurry.

The ball-millings were carried out in ethanol in order to prevent the leaching of Ba and Sr from the samples that would occur if an aqueous milling medium were used. All but the first milling (f), were carried out in an 8-inch-diameter mill, rotating at 72 rpm, using 1/2-in.-diameter balls. The weight ratios of sample: ethanol: balls were about 1 : 4 : 35. The first milling (f), which was intended only to homogenize the sample, was carried out in a 12-inch-diameter mill.

3. Fabrication

The ferrites, in the form of alcoholic slurries, were pressed under the influence of a magnetic field to form 1·5-inch-diameter disks. (9). The forming pressure was 5000 psi. The magnetic field was applied intermittently with a maximum magnetomotive force of about 30,000 amp-turns.

The "green" disks were then dried and demagnetized by heating them to 500°C. Their green densities (D_g) were determined from measurements of their dimensions and their weight.

4. Sintering

The sintering of these specimens was carried out in a large muffle furnace. Three or four equivalent disks of six batches, making 18 to 24 disks in total, were sintered at one time. The arrangement of the disks in

the furnace was such that the effects of any variations in the hot zone of the furnace would be detected. The heating rate was set at 60 deg C/hr , the soaking time was 2 hr and the furnace was cooled to room temperature at its natural cooling rate.

The diameters of the sintered disks were then measured to determine the diametral shrinkage (S_d). The disks were then lapped to perfect cylinders with their two faces parallel and their sintered densities (D_s) were determined prior to making the magnetic measurements. The parallel faces of the disks were ground with carborundum grinding compound No. 280. The faces were made parallel to within a tolerance of about $\pm$ 0·0002 inch.

It was not possible to measure the thickness shrinkage directly due to slight warping of some disks. The thickness shrinkage (S_t) was calculated as follows:

$$S_t = \left\{ 1 - \frac{D_g}{D_s} \left[\frac{1}{1 - \frac{S_d}{100}} \right]^2 \right\} \times 100$$

where S_t = thickness shrinkage in %,

D_g = green density g/cm^3,

D_s = sintered density g/cm^3,

$S_d = (1 - \phi_s/\phi_g) \times 100$

= diametrical shrinkage in %,

ϕ_g and ϕ_s = green and sintered diameters, respectively, in cm.

5. Magnetic Measurements

The magnetic properties of the specimens were measured using the "pole-coil" method (10). The lapped disks were carefully placed between the two poles so as to minimize the air gap. A schematic diagram of the arrangement of the magnetic measurement equipment is given in Figure 2. Curves of (B - H) vs H were plotted automatically. The magnetic quantities

B_r, $_iH_c$, $_bH_c$ and $(BH)_{max}$ were read or calculated graphically. No corrections were made for any possible errors due to such factors as crystallographic and/or ceramic inhomogeneity of the specimens, non-linearity of the permeability of the pole faces, etc. However, the quantities reported were obtained by averaging the measurements of three to four specimens.

RESULTS AND DISCUSSION

The chemical compositions of the end-members of this system were found to be $BaO.5{\cdot}2Fe_2O_3$ and $SrO.5{\cdot}2Fe_2O_3$, respectively (11, 12). Since the other members of this system were prepared essentially by dry-mixing appropriate amounts of these two end-members, and since alcohol was used as the mixing medium, it is justifiable to assume that there was very little or no leaching of either barium or strontium from the samples during milling; that is, the $Fe_2O_3/(Ba + Sr)O$ ratios throughout the system were constant. The composition of the mixtures in the system can therefore be expressed as $(Ba_{1-x}Sr_x)O.5{\cdot}2Fe_2O_3$. Intervals of $0{\cdot}2$ in the various values of x were studied.

The results of both the ceramic and magnetic measurements on the series of compositions are tabulated in Tables 1A to 1F and are shown graphically in Figures 3A to 3F inclusive. It must be noted here that these were the properties of the system under the particular experimental conditions described in the foregoing experimental section of this report. Recent investigations in this laboratory have shown that the operational variables, such as calcination temperature, milling time, etc., play an important role in determination of the magnetic properties of hard ferrites (13) and the conditions in the present study were not the optimum ones. The mean values listed in these tables are the arithmetic means of tests on two to four identical specimens. This repetition was carried out as a precaution against possible inhomogeneity either in the samples or in the hot zone of the furnace used. It was found that the reproducibility was very good; this can be seen from the various tables of results presented.

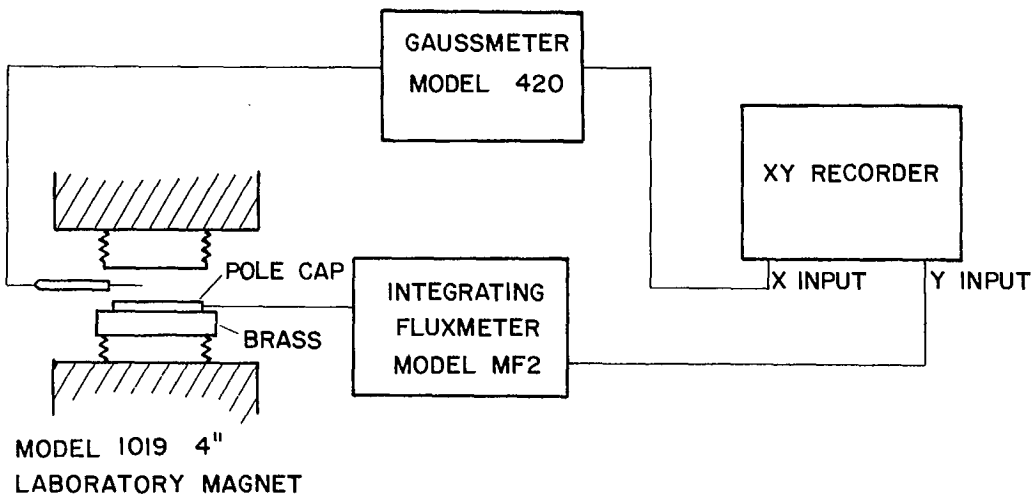

FIGURE 2 SCHEMATIC DIAGRAM OF MAGNETIC TESTING EQUIPMENT FOR BARIUM / STRONTIUM FERRITES

TABLE 1A - Ceramic and Magnetic Properties of $BaO \cdot 5 \cdot 2 Fe_2O_3$, Calcined at 1300°C for 2 hr , Ball-milled for 8 hr , and Sintered at Various Temperatures for 2 hr

Sintering Temp. (°C)	Green Density (D_g) (g/cm^3)		Sintered Density (D_s) (g/cm^3)		Diametral Shrinkage (S_d) (%)		Thickness Shrinkage (S_t) (%)		Intrinsic Coercive Force ($_iH_c$)(Oe)		Coercive Force ($_bH_c$) (Oe)		Remanent Magnetization (B_r) (G)		Energy Product $[(BH)_{max} \times 10^6]$(G.Oe)	
		Mean		Mean		Mean		Mean		Mean		Mean		Mean		Mean
1100	2.80	2.80	3.33	3.31	2.9	3.0	10.8	10.1	3233	3233	2370	2360	2550	2550	1.56	1.56
	2.81		3.31		3.0		9.8		3160		2390		2610		1.59	
	2.80		3.29		3.0		9.6		3310		2320		2490		1.54	
1130	2.82	2.84	3.52	3.53	3.9	3.8	13.3	13.1	2920	2900	2500	2440	2710	2670	1.76	1.72
	2.83		3.50		3.8		12.6		2920		2380		2590		1.63	
	2.87		3.57		3.7		13.3		2850		2450		2700		1.76	
1165	2.83	2.82	3.76	3.74	5.0	5.0	16.6	16.4	2570	2570	2450	2470	2840	2840	1.92	1.93
	2.81		3.73		5.0		16.5		2540		2470		2850		1.95	
	2.82		3.72		5.0		16.0		2600		2500		2830		1.92	
1190	2.85	2.85	4.22	4.21	6.7	6.7	22.4	22.0	1890	1890	1780	1790	3230	3260	2.45	2.47
	2.87		4.23		6.7		22.1		1890		1820		3300		2.60	
	2.86		4.21		6.7		22.0		1880		1710		3220		2.42	
	2.85		4.18		6.8		21.5		1900		1860		3200		2.40	
1230	2.85	2.83	4.97	4.98	9.7	9.7	29.7	30.3	900	900	890	890	3820	3820	2.40	2.37
	2.80		4.99		9.8		31.1		900		890		3800		2.32	
	2.83		4.99		9.7		30.2		900		890		3800		2.39	

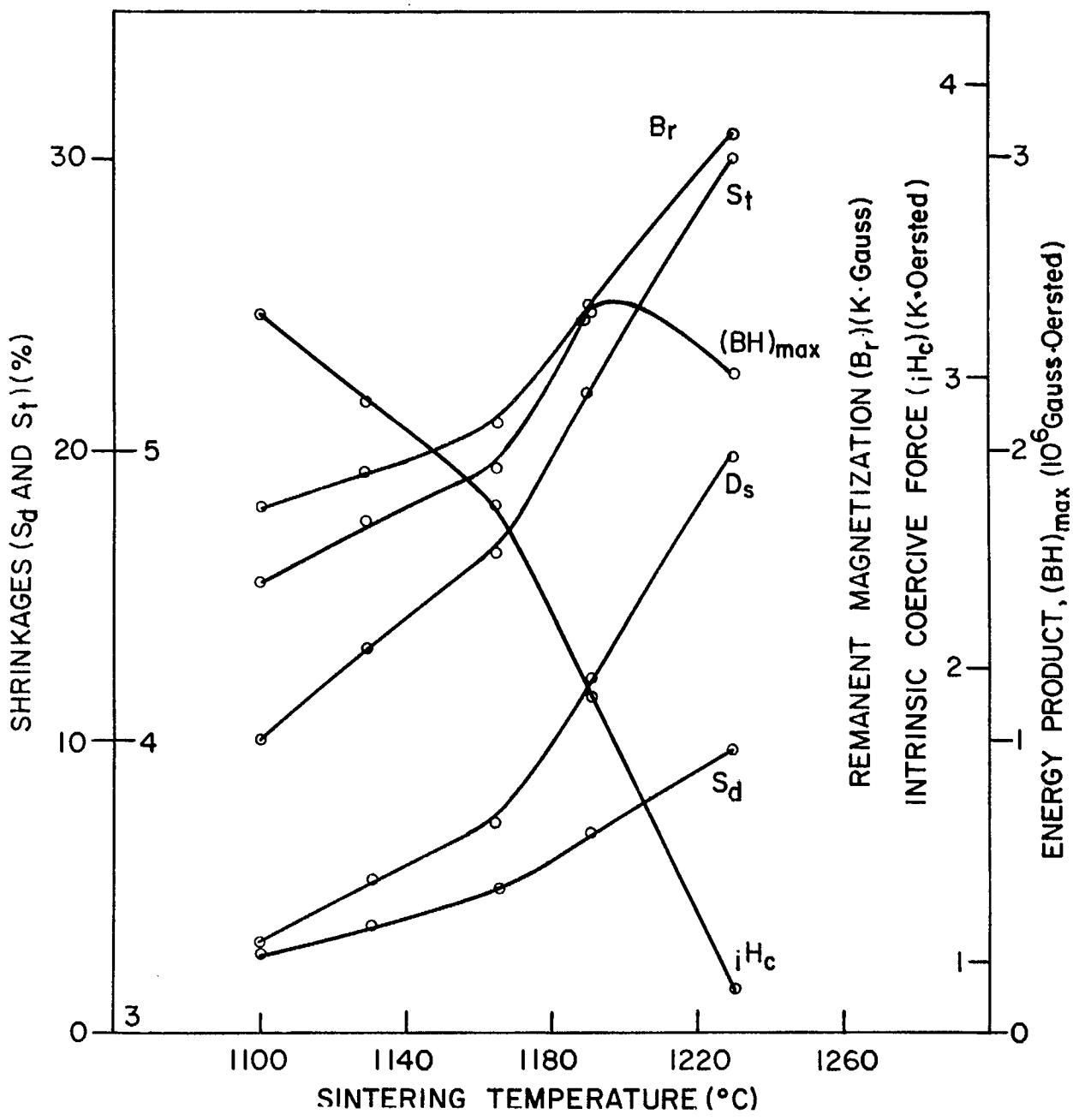

Figure 3A. Ceramic and Magnetic Properties of $BaO.5{\cdot}2Fe_2O_3$, Sintered at Various Temperatures for 2 hr.

TABLE 1B - Ceramic and Magnetic Properties of $(Ba_{0.8}Sr_{0.2})O.5{\cdot}2Fe_2O_3$, Calcined at 1300°C for 2 hr , Ball-milled for 8 hr , and Sintered at Various Temperatures for 2 hr

Sintering Temp. (°C)	Green Density (D_g) (g/cm^3)		Sintered Density (D_s) (g/cm^3)		Diametral Shrinkage (S_d) (%)		Thickness Shrinkage (S_t) (%)		Intrinsic Coercive Force $({}_iH_c)$ (Oe)		Coercive Force $({}_bH_c)$ (Oe)		Remanent Magnetization (B_r) (G)		Energy Product $[(BH)_{max} \times 10^6]$ (G.Oe)	
		Mean		Mean		Mean		Mean		Mean		Mean		Mean		Mean
1100	2.82	2.82	3.51	3.51	4.2	4.2	12.5	12.2	2800	2780	2300	2395	2610	2710	1.57	1.72
	2.84		3.51		4.2		11.9		2760		2490		2810		1.86	
1130	2.83	2.82	3.88	3.88	6.3	6.3	16.9	17.2	2250	2270	2180	2190	2820	2910	1.98	2.09
	2.82		3.88		6.2		17.4		2300		2200		3000		2.20	
1165	2.85	2.84	4.39	4.41	8.6	8.6	22.3	23.0	1480	1420	1450	1390	3490	3500	2.79	2.71
	2.83		4.40		8.5		23.2		1390		1350		3500		2.67	
	2.83		4.43		8.6		23.6		1400		1380		3500		2.68	
1190	2.83	2.84	4.89	4.91	10.6	10.7	27.6	27.4	1000	1000	960	980	3850	3920	2.40	2.54
	2.83		4.90		10.6		27.8		990		980		3840		2.40	
	2.86		4.92		10.7		27.1		1000		990		4000		2.70	
	2.85		4.91		10.7		27.2		1000		990		4000		2.80	
1230	2.82	2.83	5.10	5.10	12.2	12.1	28.3	28.1	790	830	780	820	4110	4010	2.50	2.30
	2.85		5.09		11.9		27.9		850		840		3850		2.10	
	2.83		5.10		12.2		28.0		860		840		4070		2.29	

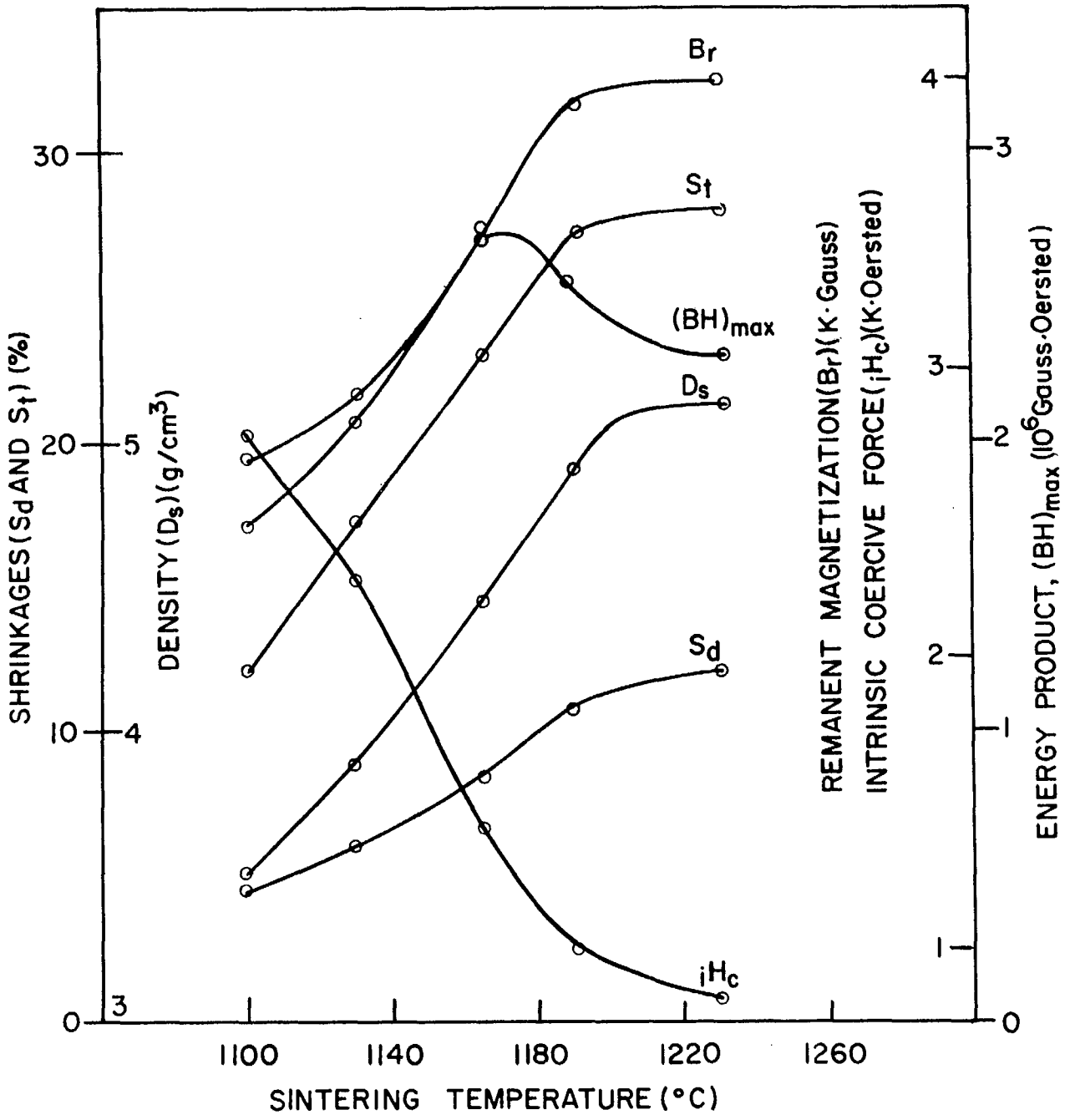

Figure 3B. Ceramic and Magnetic Properties of $(Ba_{0.8}Sr_{0.2})O.5{\cdot}2Fe_2O_3$, Sintered at Various Temperatures for 2 hr.

TABLE 1C - Ceramic and Magnetic Properties of $(Ba_{0.6}Sr_{0.4})O.5{\cdot}2\,Fe_2O_3$ Calcined at 1300°C for 2 hr, Ball-milled for 8 hr, and Sintered at Various Temperatures for 2 hr

Sintering Temp. (°C)	Green Density (D_g) g/cm^3		Sintered Density (D_s) g/cm^3		Diametral Shrinkage (S_d) (%)		Thickness Shrinkage (S_t) (%)		Intrinsic Coercive Force $({}_iH_c)$(Oe)		Coercive Force $({}_bH_c)$ (Oe)		Remanent Magnetization (B_r) (G)		Energy Product $[(BH)_{max} \times 10^6]$(G.Oe)	
		Mean		Mean		Mean		Mean		Mean		Mean		Mean		Mean
1100	2.83	2.81	3.46	3.45	4.1	4.1	11.1	11.3	3060	3040	2490	2510	2750	2770	1.80	1.83
	2.81		3.44		4.1		11.0		3040		2510		2750		1.85	
	2.80		3.45		4.1		11.8		3020		2510		2800		1.86	
1130	2.78	2.80	3.93	3.95	6.8	6.8	18.6	18.4	2180	2180	2140	2130	3110	3130	2.26	2.32
	2.79		3.95		6.8		18.7		2160		2120		3150		2.40	
	2.82		3.95		6.8		17.8		2190		2140		3120		2.31	
1165	2.81	2.80	4.55	4.56	9.6	9.6	24.5	24.8	1290	1250	1250	1220	3680	3650	2.80	2.69
	2.80		4.56		9.4		25.2		1230		1220		3710		2.78	
	2.80		4.57		9.8		24.7		1230		1200		3570		2.48	
1190	2.81	2.81	5.02	5.01	11.9	11.9	27.9	27.7	950	950	940	940	4200	4070	2.68	2.58
	2.83		5.00		11.8		27.3		970		960		4170		2.60	
	2.81		5.02		11.9		27.9		950		940		3930		2.48	
	2.80		5.01		12.1		27.7		950		950		3990		2.56	
1230	2.83	2.81	5.10	5.11	12.8	12.8	27.2	27.7	820	830	810	820	4000	4120	2.24	2.34
	2.81		5.11		12.7		27.9		820		810		4200		2.38	
	2.80		5.12		12.8		28.1		860		840		4150		2.41	

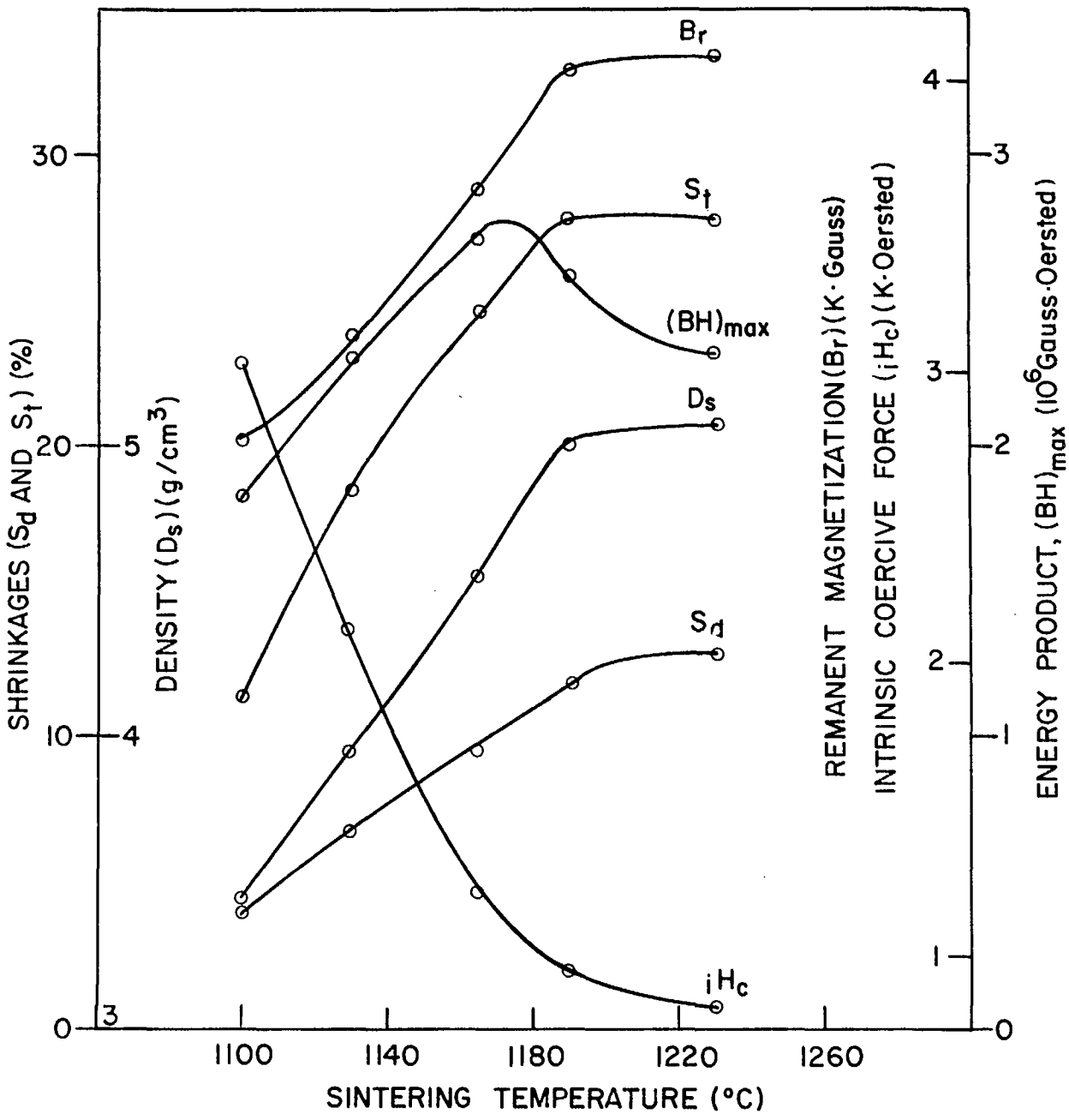

Figure 3C. Ceramic and Magnetic Properties of $(Ba_{0.6}Sr_{0.4})O.5{\cdot}2Fe_2O_3$, Sintered at Various Temperatures for 2 hr.

TABLE 1D - Ceramic and Magnetic Properties of $(Ba_{0.4}Sr_{0.6})O.5{\cdot}2\,Fe_2O_3$, Calcined at 1300°C for 2 hr, Ball-milled, for 8 hr, and Sintered at Various Temperatures for 2 hr

Sintering Temp. (°C)	Green Density (D_g) (g/cm^3)		Sintered Density (D_s) (g/cm^3)		Diametral Shrinkage (S_d) (%)		Thickness Shrinkage (S_t) (%)		Intrinsic Coercive Force $({}_iH_c)$(Oe)		Coercive Force $({}_bH_c)$ (Oe)		Remanent Magnetization (B_r) (G)		Energy Product $[(BH)_{max} \times 10^6]$(G.Oe)	
		Mean		Mean		Mean		Mean		Mean		Mean		Mean		Mean
1100	2.76	2.77	3.38	3.38	3.9	4.0	11.6	11.2	3150	3180	2500	2510	2750	2700	1.85	1.80
	2.77		3.37		4.1		10.6		3250		2510		2700		1.78	
	2.78		3.40		3.9		11.5		3150		2510		2600		1.77	
1130	2.78	2.80	3.89	3.89	6.7	6.7	17.9	17.5	2310	2300	2270	2250	3110	3050	2.26	2.24
	2.2		3.90		6.7		17.0		2300		2220		2900		2.10	
	2.79		3.89		6.7		17.6		2300		2250		3150		2.37	
1165	2.76	2.76	4.57	4.58	10.0	10.1	25.5	25.4	1220	1210	1200	1200	3675	3680	2.75	2.74
	2.76		4.58		10.1		25.5		1200		1210		3710		2.80	
	2.77		4.58		10.1		25.2		1200		1190		3670		2.68	
1190	2.75	2.76	5.01	5.01	12.3	12.2	28.2	28.4	900	900	890	890	4200	4090	2.56	2.55
	2.78		5.01		12.1		28.2		900		890		3950		2.40	
	2.76		5.01		12.3		28.4		900		890		4210		2.68	
	2.77		5.02		12.2		28.4		920		900		4010		2.56	
1230	2.77	2.76	5.07	5.08	13.2	13.2	27.5		910	910	900	900	3940	4080	2.25	2.46
	2.76		5.08		12.2		27.9		900		890		4150		2.60	
	2.76		5.08		13.2		27.9		910		900		4150		2.54	

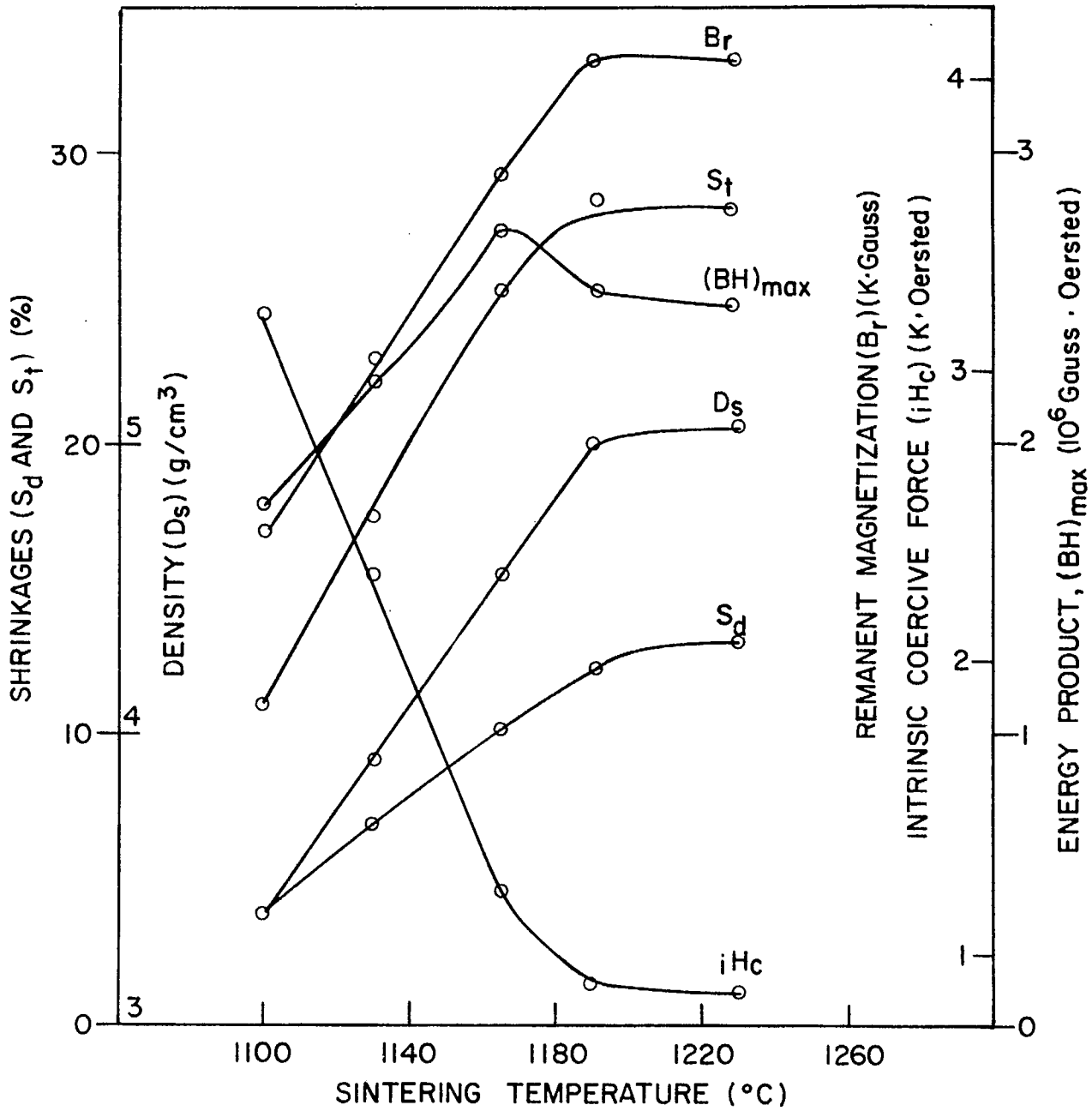

Figure 3D. Ceramic and Magnetic Properties of $(Ba_{0.4}Sr_{0.6})O.5{\cdot}2Fe_2O_3$, Sintered at Various Temperatures for 2 hr.

TABLE 1E - Ceramic and Magnetic Properties of $(Ba_{0.2}Sr_{0.8})O.5{\cdot}2\ Fe_2O_3$, Calcined at 1300°C for 2 hr, Ball-milled for 8 hr, and Sintered at Various Temperatures for 2 hr

Sintering Temp. (°C)	Green Density (D_g) (g/cm^3)		Sintered Density (D_s) (g/cm^3)		Diametral Shrinkage (S_d) (%)		Thickness Shrinkage (S_t) (%)		Intrinsic Coercive Force ($_iH_c$)(Oe)		Coercive Force ($_bH_c$) (Oe)		Remanent Magnetization (B_r) (G)		Energy Product $[(BH)_{max} \times 10^6]$ (G.Oe)	
		Mean		Mean		Mean		Mean		Mean		Mean		Mean		Mean
1100	2.71	2.71	3.40	3.39	4.2	4.2	13.2	13.0	3220	3280	2510	2510	2700	2690	1.74	1.74
	2.69		3.40		4.2		13.8		3250		2520		2710		1.79	
	2.73		3.38		4.2		12.0		3360		2510		2650		1.69	
1130	2.70	2.71	3.96	3.93	7.1	7.1	21.0	20.3	2360	2360	2300	2300	2990	3040	2.06	2.19
	2.72		3.93		7.1		19.8		2370		2300		3110		2.32	
	2.70		3.91		7.1		20.0		2360		2300		3010		2.18	
1165	2.69	2.70	4.60	4.61	10.3	10.4	27.3	27.1	1240	1223	1220	1230	3750	3750	2.86	2.87
	2.69		4.63		10.5		27.5		1250		1240		3750		2.88	
	2.71		4.60		10.5		26.5		1240		1220		3750		2.86	
1190	2.72	2.70	5.00	5.01	12.6	12.6	28.8	29.5	950	960	940	950	4250	4250	2.80	2.75
	2.70		5.01		12.5		29.6		1010		1000		4290		2.80	
	2.71		5.02		12.4		29.7		950		940		4200		2.72	
	2.68		5.01		12.7		29.8		950		920		4250		2.69	
1230	2.69	2.69	5.03	5.02	13.1	13.1	29.2	29.2	1060	1060	1050	1040	3950	4010	2.70	2.77
	2.69		5.03		13.1		29.2		1080		1040		4110		2.88	
	2.69		5.02		13.1		29.2		1050		1030		3960		2.77	

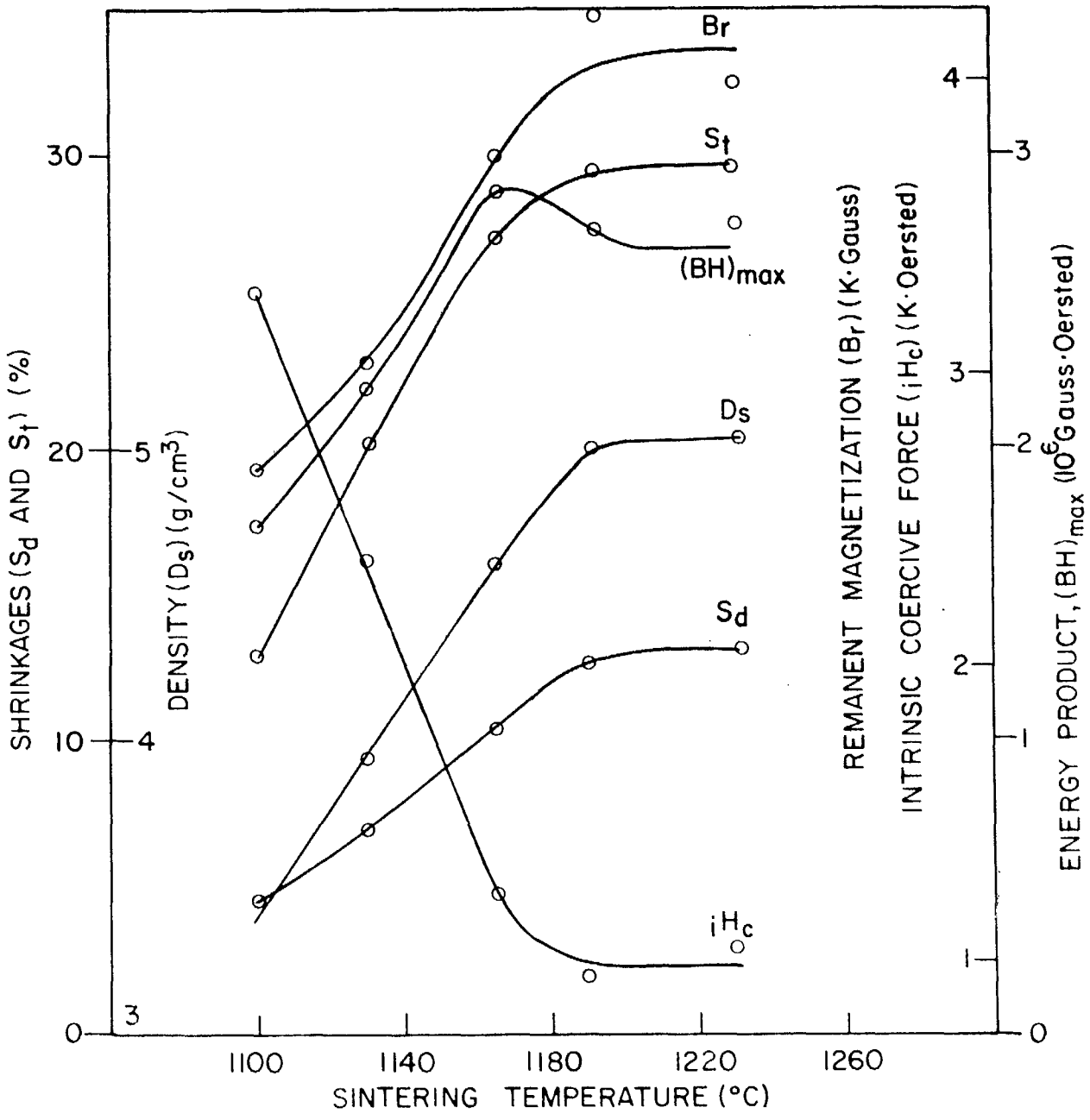

Figure 3E. Ceramic and Magnetic Properties of $(Ba_{0.2}Sr_{0.8})O.5{\cdot}2Fe_2O_3$, Sintered at Various Temperatures for 2 hr.

TABLE 1F - Ceramic and Magnetic Properties of SrO. 5-2 Fe_2O_3, Calcined at 1300°C for 2 hr, Ball-milled for 8 hr, and Sintered at Various Temperatures for 2 hr

Sintering Temp. (°C)	Green Density (D_g) (g/cm^3)		Sintered Density (D_g) (g/cm^3)		Diametral Shrinkage (S_d) (%)		Thickness Shrinkage (S_t) (%)		Intrinsic Coercive Force ($_iH_c$)(Oe)		Coercive Force ($_bH_c$) (Oe)		Remanent Magnetization (B_r) (G)		Energy Product $[(BH)_{max} \times 10^6]$(G.Oe)	
		Mean		Mean		Mean		Mean		Mean		Mean		Mean		Mean
1100	2.61	2.61	3.39	3.39	5.1	5.2	14.5	14.4	3700	3700	2520	2547	2690	2720	1.71	1.76
	2.61		3.39		5.2		14.4		3690		2520		2720		1.74	
	2.62		3.40		5.2		14.3		3700		2600		2750		1.84	
1130	2.62	2.61	3.98	3.97	8.1	8.1	22.1	22.4	2780	2790	2680	2680	3020	2010	2.26	2.23
	2.60		3.98		8.1		22.7		2800		2670		3020		2.22	
	2.61		3.97		8.0		22.4		2800		2700		3000		2.23	
1165	2.60	2.61	4.60	4.62	11.1	11.2	28.5	28.4	1640	1630	1610	1600	3800	3770	3.38	3.31
	2.62		4.61		11.1		28.1		1590		1570		3760		3.25	
	2.60		4.64		11.4		28.6		1650		1620		3750		3.30	
1190	2.64	2.63	4.96	4.96	12.2	12.4	31.0	31.0	1000	1030	980	1010	4030	4040	2.50	2.61
	2.63		4.96		12.2		31.2		1130		1090		4150		2.63	
	2.62		4.96		12.6		30.9		1000		990		4020		2.68	
	2.62		4.96		12.6		30.9		1000		980		4010		2.65	
1230	2.61	2.61	5.01	5.00	14.0	14.0	29.5	29.5	980	970	960	940	4050	4040	2.55	2.40
	2.60		5.00		13.9		29.9		930		910		3910		2.18	
	2.62		5.00		14.1		29.0		990		960		4150		2.56	

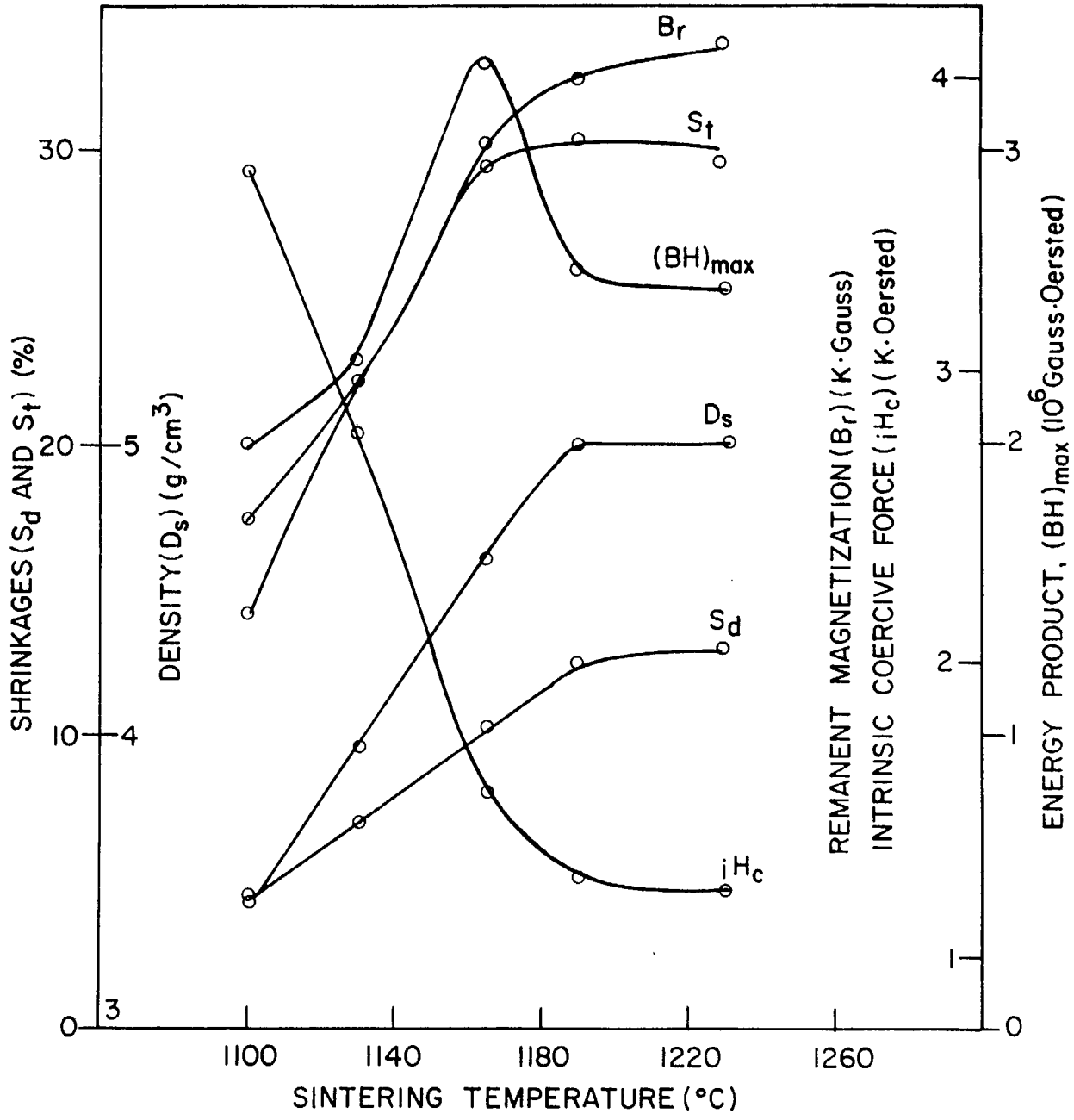

Figure 3F. Ceramic and Magnetic Properties of SrO. 5·2Fe_2O_3, Sintered Various Temperatures for 2 hr.

1. Density and Shrinkages

It has been previously mentioned that the specimens in this system all have the chemical composition $(Ba_{1-x}Sr_x)O.5\cdot2Fe_2O_3$. The stoichiometric composition of the hexaferrites is $MO.6\cdot0Fe_2O_3$. There is a difference of opinion in the literature concerning the range of non-stoichiometry that $BaO.6\cdot0Fe_2O_3$ and $SrO.6\cdot0Fe_2O_3$ can tolerate in terms of MO/Fe_2O_3 ratio, while still retaining the hexaferrite crystallographic structure. Goto and Takada (14) reported that there was a considerable range of non-stoichiometry in the $BaO-Fe_2O_3$ system is this regard. However, van Hook (15) has denied this and claims that the range of non-stoichiometry of the barium hexaferrite is either very narrow or even non-existent. In the case of the strontium hexaferrite, the matter is even more uncertain. The phase diagram for the $SrO-Fe_2O_3$ system published by Batti (16) does not indicate any range of non-stoichiometry for strontium hexaferrite.

If we consider, then, that the tolerated range of non-stoichiometry is either narrow or non-existent for both hexaferrites, then our specimens, having the compositions as indicated above, must, therefore, contain at least one other phase. In the case of the pure barium compound, it is probable that the second phase would be $BaFe_2O_4$ (i.e., $BaO.Fe_2O_3$)(14). In the case of the pure strontium specimens, it is probable that the second phase would be $7SrO.5Fe_2O_3$ (16). In the case of the mixed barium-strontium specimens, there could very well be two minor phases present (17). In any case, however, the foreign phase(s) would be present only to an amount of the order of 5% of the total composition. In those cases where data are available, it will be observed that the densities of the foreign phases are very similar to those of their corresponding stoichiometric hexaferrites. Further, the lattice constants of both barium and strontium hexaferrites are essentially the same. For these reasons it is considered justifiable to assume that the X-ray densities of specimens in this system would be the same as if the specimens consisted entirely of the respective stoichiometric hexaferrites, $(Ba_{1-x}Sr_x)O.6\cdot0Fe_2O_3$, and would vary linearly with x across

the system from $BaO.6{\cdot}0Fe_2O_3$ to $SrO.6{\cdot}0Fe_2O_3$. This assumption was made in calculating the X-ray densities of the samples.

The relative density, i.e., the ceramic density divided by the X-ray density of the same sample, as a function of the composition, is shown in Figure 4. It can be seen that the relative green density seems to be almost independent of the composition, varying only between 50 and 53%. The variation of the sintered density with sintering temperature is plotted, together with the magnetic properties, in Figures 3A to 3F, inclusive. The sintering temperature was varied up to 1230°C. At this temperature, the coercive force of all the samples was sufficiently low that there would be no advantage to sinter to higher temperatures.

The density of all the samples, with the exception of that of the pure barium ferrite, behaved in more or less the same way. It increased almost linearly as the sintering temperature was increased up to a certain point, beyond which the density changed very slowly with sintering temperature. This point occured at a relative density of about 98-99%. The pure barium ferrite samples behaved differently from the others. The sintered density in this case increased relatively slowly with temperature up to about 1160°C, and then increased at a faster rate at temperatures higher than 1160°C. Figure 4 shows that only a small amount of strontium was needed to mask this different behaviour of barium ferrite. For $x > 0{\cdot}2$, the densification behaviour was very similar for all samples.

These specimens all showed very strong anisotropic shrinkage behaviour. The shrinkage ratio (S_t/S_d) varied from 2·1 to 3·6 (see Table 2). Generally, the shrinkage ratio decreased as the sintering temperature was increased.

2. Magnetic Properties

The remanent magnetization, B_r, (see Figures 3A to 3F, inclusive) behaved as expected. It increases with sintering temperature in the same manner as the density. The corrected values of $B_r/B_{r_{100}}$, namely, (the value of B_r when the density has been corrected to 100%) where

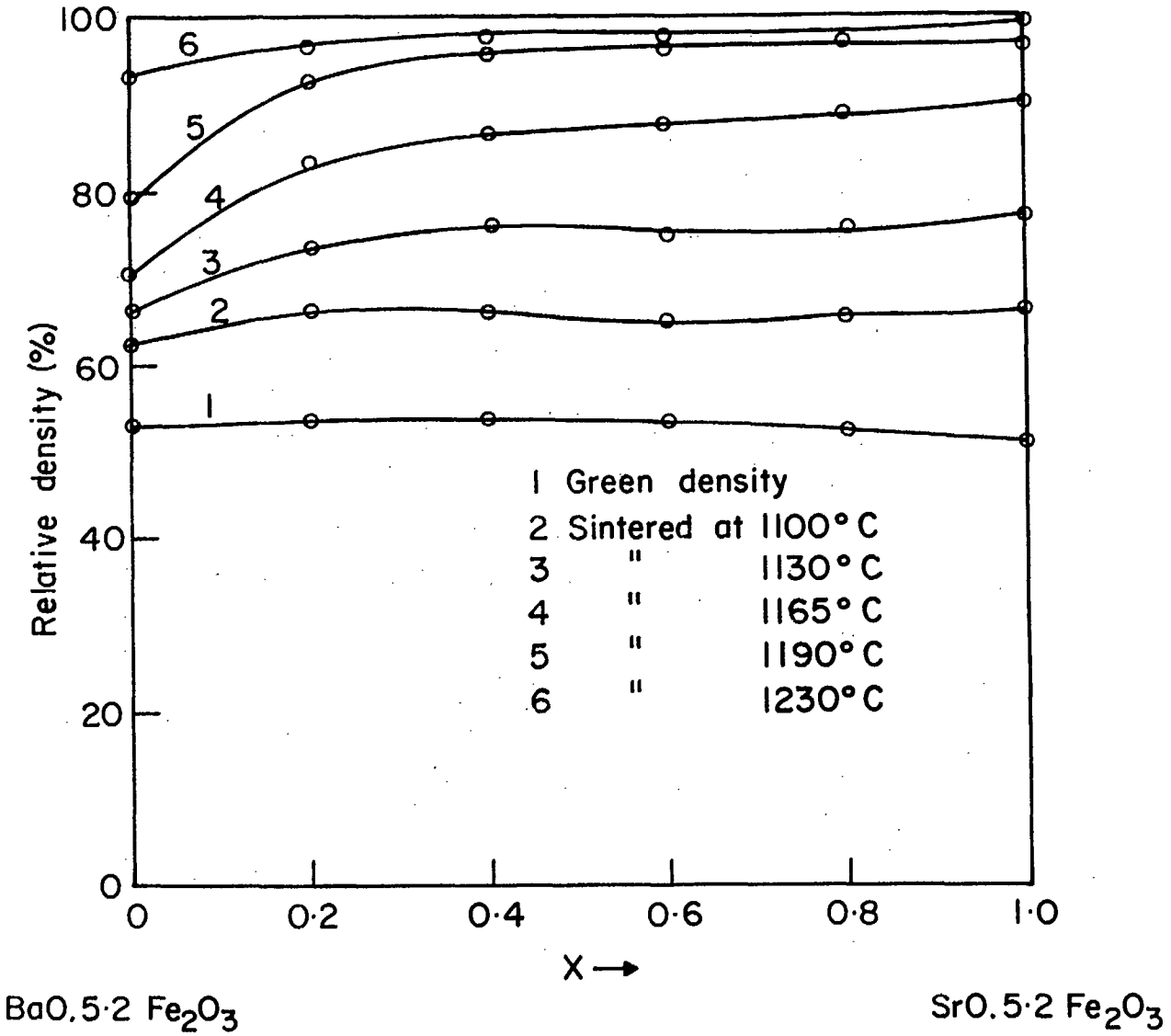

Figure 4. Relative Sintered Density of $(Ba_{1-x}Sr_x)O.5{\cdot}2Fe_2O_3$, Sintered for 2 hr at Various Temperatures.

TABLE 2 - Ratio of Thickness Shrinkage to Diametral Shrinkage (S_t/S_d) for $(Ba_{1-x}Sr_x)O.5{\cdot}2\,Fe_2O_3$

Sintering Temp. °C	COMPOSITION											
	x = 0		x = 0.2		x = 0.4		x = 0.6		x = 0.8		x = 1.0	
	S_t/S_d	Mean*	S_t/S_d	Mean	S_t/S_d	Mean	S_t/S_d	Mean	S_t/S_d	Mean	S_t/S_d	Mean
1100	3.72		2.97		2.70		2.97		3.14		2.84	
	3.27	3.40	2.83	2.90	2.61	2.73	2.58	2.83	2.28	3.09	2.76	2.78
	3.20				2.87		2.94		2.85		2.75	
1130	3.41		2.68		2.73		2.67		2.95		2.72	
	3.31	3.44	2.80	2.74	2.75	2.70	2.53	2.61	2.78	2.85	2.80	2.77
	3.59				2.61		2.62		2.81		2.80	
1165	3.32		2.59		2.55		2.55		2.65		2.57	2.45
	3.30	3.27	2.72	2.68	2.68	2.58	2.52	2.52	2.60	2.53	2.54	
	3.20		2.74		2.52		2.49		2.52		2.51	
1190	3.34		2.60		2.34		2.31		2.28		2.54	
	3.29	3.27	2.62	2.57	2.31	2.32	2.33	2.32	2.37	2.35	2.56	2.50
	3.28		2.53		2.31		2.31		2.39		2.45	
	3.16		2.54		2.34		2.33		2.35		2.45	
1230	3.06		2.32		2.12		2.08		2.23		2.11	2.11
	3.17	3.11	2.34	2.32	2.20	2.17	2.11	2.10	2.23	2.23	2.11	
	3.11		2.29		2.19		2.11		2.23		2.06	

*Mean: Arithmetic mean of (S_t/S_d).

$B_{r_{100}} = B_r / d_{relative}$ are listed in Table 3.

It can be seen from this table that $B_{r_{100}}$ is essentially constant. Hence, the increase in the remanent magnetization with increasing sintering temperature is essentially the result of densification of the specimens. Any substantial improvement in the degree of orientation only occurs at the initial stage of sintering. There is no evidence of improvement in the degree of orientation over the range of sintering temperatures used in this work. The squareness of the hysteresis curves, however, showed substantial improvement with increasing sintering temperatures. This improvement may be mainly due to the disappearance of pores, which have a demagnetizing effect, lattice defects, etc., rather than to an improvement in degree of orientation. This assumption is based on the phenomenon observed by Richter (6). He observed a lowering of the magnetic moment of a powder when it was subjected to extensive milling, a process which is known to introduce strain and lattice defects.

The intrinsic coercive force behaved as expected. It decreases as the sintering temperature is increased. As is shown in Figure 5, this decrease in the intrinsic coercive force appears to be approximately linear with respect to the increase in density. With the exception of the pure strontium composition ($x = 1$), all the points seem to fall on one straight line, especially those corresponding to relative densities of less than 90%. Pure strontium ferrite shows a higher intrinsic coercive force, but still yields a straight line of approximately the same slope. The least-squares fits of these lines are:

$$ {}_iH_c = -81.8\, d + 8394 \quad \text{with} \quad \delta = 109 $$

$$ \text{for} \quad x \leq 0.8 \quad \text{and} \quad d < 90 $$

and

$$ {}_iH_c = -84.6\, d + 9296 \quad \text{with} \quad \delta = 63 $$

$$ \text{for } x = 1 \text{ and } 60 < d < 100 $$

TABLE 3 - Relative Remanent Magnetization* of $(Ba_{1-x}Sr_x)O.5 \cdot 2\,Fe_2O_3$

Sintering Temp. (°C)	COMPOSITION					
	x = 0	x = 0.2	x = 0.4	x = 0.6	x = 0.8	x = 1.0
1100	4093	4075	4205	4160	4102	4121
1130	4015	3959	4153	4087	3995	3900
1165	4034	4192	4195	4192	4209	4193
1190	4114	4217	4259	4254	4385	4184
1230	4080	4151	4223	4191	4122	4129

*Relative Remanent Magnetization = $B_{r_{100}} = \frac{B_r}{d}$,

Where d = relative density

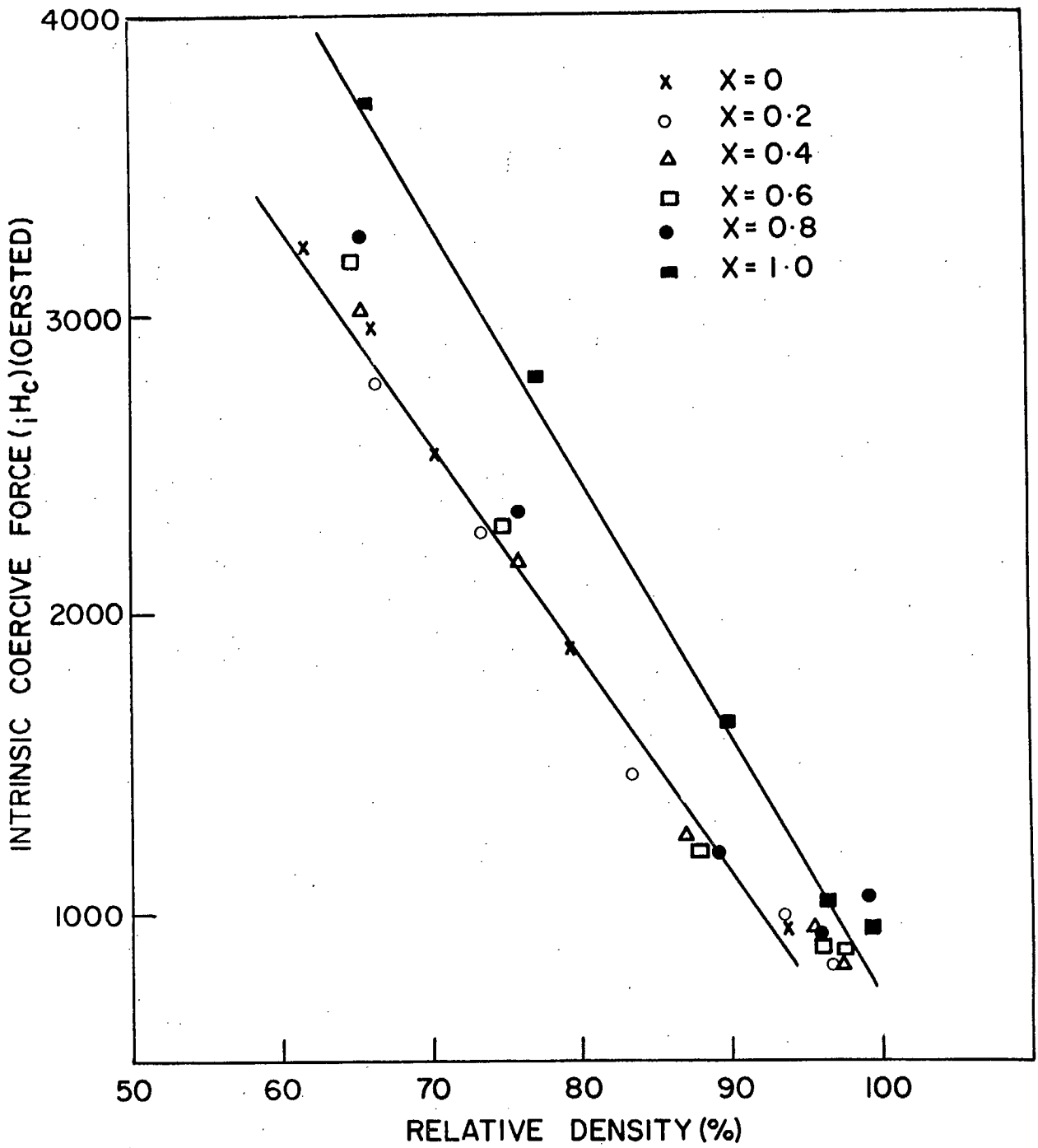

Figure 5. Intrinsic Coercive Force vs. Relative Density of $(Ba_{1-x}Sr_x)O.5{\cdot}2Fe_2O_3$, Calcined at 1300°C for 2 hr, Ball-Milled for 8 hr, and Sintered at Various Temperatures for 2 hr.

where:

$_{i}H_{c}$ = intrinsic coercive force in oersted,

d = relative density in %,

x = mole fraction of strontium ferrite,

$$\delta = \sqrt{\frac{\sum (_{i}H_{c} - _{i}H_{c}\ \text{calc})}{k - 1}},$$

and k = number of experimental points.

The ratio of the coercive force, $_{b}H_{c}$, to the intrinsic coercive force, $_{i}H_{c}$, (Table 4), which is one of the measures of the quality of the hysteresis curve of a specimen, is generally in the order of 96 to 99%, with the exception of those specimens with a very low remanent magnetization. For the latter specimens, the values of $_{i}H_{c}$ are larger than the values of B_{r} and, consequently, the ratio of these two coercive forces does not measure the quality of the hysteresis curves.

As expected from the ceramic properties of these specimens, the optimum sintering temperature, from the point of view of the maximum energy product, $(BH)_{max}$, does not vary greatly over the range of specimens studied. This optimum occurred at about 1150°C, with the exception of pure barium ferrite, for which it occurred at about 1185°C. The optimumvalues of the maximum energy product, $(BH)_{max}$, are plotted against the composition in Figure 6. It can be seen that the optimum values of the maximum energy product vary from 2.5×10^{6} gauss-oersted for pure barium ferrite to 3.3×10^{6} gauss-oersted for pure strontium ferrite. These values are low in comparison with best values that can be attained with both of these materials with doping and with undoped materials under different treatments (13). The first situation was obviously caused by the absence of grain-growth inhibitors and the second was caused by the choice of the technological variables which, in the later phases of the work in this laboratory, have been found to be very important factors (13).

TABLE 4 - Ratio of Coercive Forces $_bH_c/_iH_c$ for $(Ba_{1-x}Sr_x)O.5{\cdot}2\,Fe_2O_3$ at Various Sintering Temperatures

Sintering Temp. (°C)	COMPOSITION (x)					
	0	0.2	0.4	0.6	0.8	1.0
1100	0.73	0.86	0.83	0.79	0.77	0.69
1130	0.80	0.96	0.98	0.97	0.97	0.96
1165	0.96	0.98	0.98	0.99	0.99	0.98
1190	0.95	0.98	0.99	0.99	0.98	0.98
1230	0.99	0.98	0.98	0.99	0.98	0.97

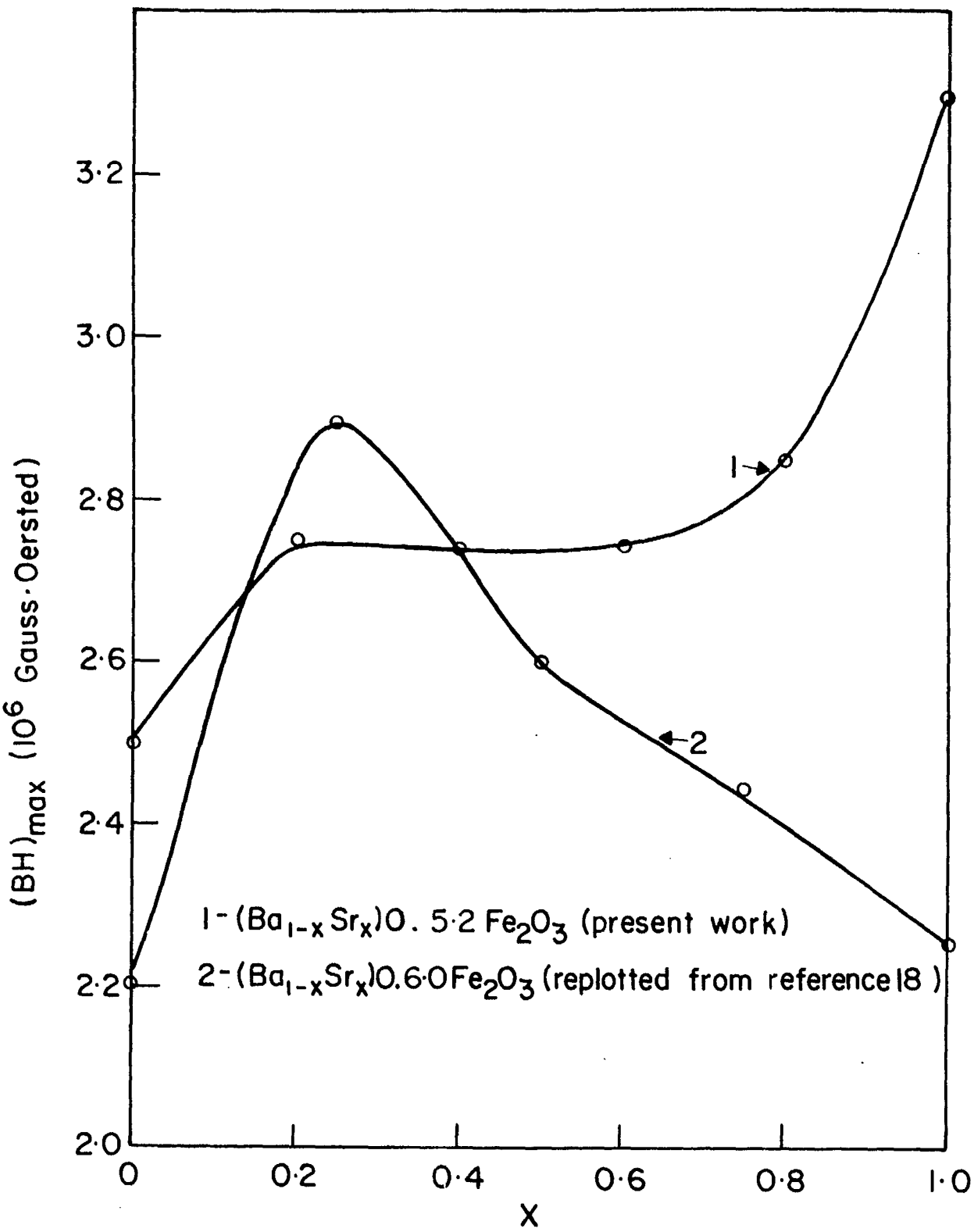

Figure 6. Energy Product $(BH)_{max}$ vs. Composition of $(Ba_{1-x}Sr_x)O.5{\cdot}2Fe_2O_3$ at their Optimum Sintering Temperatures.

The value of $(BH)_{max}$ for barium ferrite was lower than that for strontium ferrite. This is not unexpected since strontium ferrite has a higher anisotropic energy. The mixed-composition specimens, however, seem to exhibit a somewhat different behaviour. Their $(BH)_{max}$ values lie between the barium and strontium values, but they are virtually independent of the barium to strontium ratio. No explanation can be offered at this time for the cause of this unexpected lack of dependence upon composition.

There is a substantial difference between curve #1 (present work) and curve #2 (data replotted from Borovik)(18) in Figure 7, both in the values of the energy product and in their trends with respect to varying composition. Borovik obtained the optimum $(BH)_{max}$ value by sintering his specimens at 1230°C for 1 hr. This is almost 90°C higher than the optimum sintering temperature obtained in the present work. This is a very large difference, even though Borovik's soaking time was half that used in the present work. It is very difficult, at present, to pin-point the exact cause of these differences since both the method of preparation and the Fe_2O_3/MO ratio were different from those used in this laboratory.

CONCLUSIONS

From the foregoing discussion, the following conclusions can be drawn:

1. The relative green density of the specimens seem to be independent of the Ba/Sr ratio. The barium ferrite specimens sintered at a higher temperature than their strontium counterparts. Mixed barium-strontium specimens, containing 20% or more strontium ferrite, behave in a manner similar to pure strontium ferrite.
2. The anisotropic properties of the hexaferrite disks were shown to vary strongly not only in their magnetic properties, but also in their ceramic properties. The ratio of the thickness to the diametral shrinkage (S_t/S_d) varies from 2.1 to 3.6. The understanding of this anisotropic behaviour is very important from the fabrication point of view.

3. The magnetic properties of the individual sample compositions behaved as expected from their ceramic properties. The coercive force of all the samples was generally low. This was partly caused by insufficient milling time.
4. The pure strontium ferrite composition behaved somewhat differently from the mixed Ba-Sr compositions. It exhibited higher coercive force at a given density; consequently, it had higher energy products than other compositions. The coercive force of all the compositions, other than pure strontium ferrite, exhibited a straight line when plotted against relative density (up to 95% density). The coercive force of strontium ferrite specimens lay on a different straight line, but with similar slope.
5. The maximum energy products obtained in this work (with the process conditions as described in the experimental section) was 2.5×10^6 gauss-oersted for pure barium ferrite and 3.3×10^6 gauss-oersted for pure strontium ferrite. The energy products of samples of mixed Ba-Sr compositions fell between the above values, but the relationship between the energy product and the composition was not linear. This relationship was found to have different trends from those reported by Borovik (see Figure 7).
6. Contrary to the previously reported work by Borovik, pure strontium ferrite seems to have the best properties. This behaviour is caused not only by the fact that it has about 10% more anisotropic energy, but also that it sinters at a lower temperature than barium ferrite.

ACKNOWLEDGEMENTS

This work was conducted under the direction of Dr. N.F.H. Bright, Head, Physical Chemistry Section, and was supported in the early stages partly by the Defence Research Board of Canada under E.C.R.D.C. Project C-73.

The lapping of the disks in preparation for making the magnetic measurements was carried out by the Preparation and Properties of Materials Section, Mineral Processing Division.

The authors would like to thank Dr. A.H. Webster for his valuable discussions throughout the period of the work and Mr. G.A.C. Wills for his experimental assistance.

The above-mentioned personnel are all members of the staff of the Mineral Sciences Division, Mines Branch.

REFERENCES

1. A.L. Stuijts et al., "Ferroxdure II and III. Anisotropic Permanent Magnet Materials", Philips Tech. Rev., 16, 141-147 (1954).
2. Sutarno and W.S. Bowman, "Ferrites: Part I. Literature Survey on Permanent-Magnet-Type Ferrite Technology", Mines Branch Investigation Report IR 67-56, August 10, 1967.
3. Rola Company (Australia) Propriety Ltd., "Method of Producing a Permanent Magnet Material", British Patent 1,022,969, March 16, 1966.
4. A.L. Stuijts, "Sintering of Ceramic Permanent Magnetic Materials", Trans. Brit. Ceram. Soc., 35, 57-74 (1956).
5. T.H. Maurer and H.G. Richter, "Effect of Milling Methods on Barium Ferrite Powder for the Production of Permanent Magnets", Powder Metallurgy, 9 [18], 151-62 (1966).
6. H.G. Richter and H.E. Dietrich, "On the Magnetic Properties of Fine-Milled Barium and Strontium Ferrite", I.E.E.E. Transactions on Magnetics, Mag-4 [2], 263-67 (1968).
7. C.S. Brown, "The Effect of Ceramic Technology on the Properties of Ferrites", Proc. Brit. Ceram. Soc., 19 [2], 55-72 (1964).
8. A.I. Vogel, "A Text-book of Quantitative Inorganic Analysis", published by John Wiley and Sons, New York, 3rd Ed. (1961).
9. Sutarno, W.S. Bowman, J.F. Tippins, and G.E. Alexander, "Ferrites: Part III. Construction and Operation of a Magnetic Orienting Press for the Fabrication of Anisotropic Ferrite Magnets", Mines Branch Investigation Report IR 67-46, May 15, 1967.

10. E. Steingroever, "Ein Magnetstahlprüfer mit richtkraftkompensiertem Flussmesser", Archiv für Elektrotechnik, 40, 275-279 (1952).

11. Mineral Sciences Division, Analytical Chemistry Subdivision, Internal Report MS-AC-67-648, July 26, 1967.

12. Ibid., Internal Report MS-AC-67-709, August 11, 1967.

13. Sutarno, W.S. Bowman, G.E. Alexander and J.D. Childs, "The Effect of Some Operational Variables on the Properties of Strontium Hexaferrite", MS-PP 69-1, Jan. 6, 1969. Submitted to the Journal of the Canadian Ceramic Society.

14. Y. Goto and T. Takada, "Phase Diagram of the System BaO-Fe_2O_3 ", Journ. Amer. Ceram. Soc., 43 [3], 150-53 (1960).

15. H.J. Van Hook, "Thermal Stability of Barium Ferrite ($BaFe_{12}O_{19}$)", Journ. Amer. Ceram. Soc., 47, [11], 579-81 (1964).

16. P. Batti, "Diagramma D'Equilibrio Del Sistema SrO-Fe_2O_3", Annali di Chimica, 52, 941-61 (1962).

17. P. Batti, "Ricerche Su Una Zona Del Sistema Ternario BaO-SrO-Fe_2O_3", Annali di Chimica, 52, 1227-47 (1962).

18. Y.S. Borovik and N.G. Yakovleva, "Influence of Texture on the Magnetic Properties of Mixed Barium and Strontium Ferrites", Fiz. Metal. Metalloved., 14 [6], 927-30, 1962.

S/WSB/GEA/pg